International Journal of Cardiology 212 (2016) 84–91

Contents lists available at ScienceDirect

International Journal of Cardiology

journal homepage: www.elsevier.com/locate/ijcard

Intravenous iron sucrose reverses anemia-induced cardiac remodeling, prevents myocardial fibrosis, and improves cardiac function by attenuating oxidative/nitrosative stress and inflammation

Jorge E. Toblli [a,*], Gabriel Cao [a], Carlos Rivas [a], Jorge F. Giani [b], Fernando P. Dominici [c]

[a] Laboratory of Experimental Medicine, Hospital Alemán, School of Medicine, University of Buenos Aires. CONICET, Av. Pueyrredon 1640, 1118 Buenos Aires, Argentina
[b] Departments of Biomedical Sciences and Pathology and Laboratory Medicine, Cedars-Sinai Medical Center, Los Angeles, CA, United States
[c] Instituto de Química y Fisicoquímica Biológicas (UBA-CONICET), Facultad de Farmacia y Bioquímica, Universidad de Buenos Aires, Buenos Aires, Argentina

ARTICLE INFO

Article history:
Received 22 December 2015
Received in revised form 7 March 2016
Accepted 13 March 2016
Available online 17 March 2016

Keywords:
Cardiac remodeling
Cardiac function
Intravenous iron sucrose
Oxidative stress
Rat

ABSTRACT

Background: According to recent clinical trial data, correction of iron deficiency with intravenous (i.v.) iron has favorable outcomes on cardiac function. We evaluated whether i.v. iron treatment of anemic rats has favorable effect on the left ventricular (LV) performance and remodeling and the role of oxidative/nitrosative stress and inflammation in the process.

Methods: After weaning, Sprague–Dawley rats were fed low iron diet for 16 weeks, after which the treatment group received five weekly doses of i.v. iron sucrose (10 mg Fe/kg body weight). Echocardiography of LV was performed and hematology parameters were assessed before treatment (baseline, day 0) and at the end of the study (day 29). On day 29, rats were sacrificed and extracellular expansion and fibrosis in LV and interventricular septum were evaluated together with oxidative/nitrosative stress, pro-inflammatory, and repair process markers.

Results: Although iron sucrose treatment did not fully correct the anemia, it reversed anemia-induced cardiac remodeling as indicated by echocardiographic and tissue Doppler parameters. Treatment with iron sucrose also prevented anemia-induced myocardial fibrosis as indicated by extracellular expansion and fibrosis markers. Anemia-induced inflammation was prevented by iron sucrose as indicated by the levels of proinflammatory (TNF-α, NF-κB_{65}) and repair process markers (HSP27, HSP70). In addition, iron sucrose treatment significantly reduced ($p < 0.01$) anemia-induced oxidative and nitrosative stress.

Conclusion: Intravenous iron sucrose treatment reversed anemia-induced remodeling of LV, prevented myocardial fibrosis, and improved cardiac function by attenuating oxidative/nitrosative stress and inflammation in the heart.

1. Background and introduction

Iron deficiency (ID) is one of the world's most prevalent nutrient deficiencies [1]. Untreated ID can lead to iron deficiency anemia (IDA), a condition in which the number of circulating red blood cells and the level of hemoglobin (Hb) are below normal values [2,3]. Moreover, irrespective of concomitant anemia, ID is a complication of many chronic diseases, such as inflammatory bowel disease, Parkinson's disease, rheumatoid arthritis, and chronic kidney disease (CKD) [4] as well as a frequent co-morbidity in heart failure (HF) patients [5]. Iron deficiency is not only an etiological factor leading to and/or aggravating anemia in HF, but it is also considered as a separate condition with unfavorable clinical and prognostic consequences [5]. Iron plays a crucial role in cardiac muscle metabolism and mitochondrial function. Therefore, it is not surprising that both IDA and ID correlate with left ventricular (LV) hypertrophy, dilatation, compromised hemodynamics and symptomatic HF [5]. Moreover, nonclinical studies have also shown that IDA causes diastolic dysfunction and heart failure with pulmonary congestion, cardiac fibrosis, and increased cardiac inflammation [6].

The mechanisms contributing to the development and progression of LV failure are not yet fully elucidated [7]. Clinical and nonclinical

Abbreviations: CKD, chronic kidney disease; Cu,Zn-SOD, Cu,Zn superoxide dismutase; FS, fractional shortening; Hb, hemoglobin; HF, heart failure; GPx, glutathione peroxidase; GSH, glutathione; HO-1, heme oxygenase-1; HSP, heat shock protein; ID, iron deficiency; IDA, iron deficiency anemia; iNOS, inducible nitric oxide synthase expression; IS, iron sucrose; IVS, interventricular septum; LV, LVDd, left ventricular left ventricular end-diastolic dimension; LVSd, left ventricular end-systolic dimension; LVPW, left ventricular posterior wall in diastole; MDA, malondialdehyde; NF-KB, nuclear factor kappa beta; $ONOO^-$, peroxynitrite; RNS, reactive nitrogen species ROS, reactive oxygen species; TBARS, thiobarbituric acid reactive species; TNF, tumor necrosis factor; TSAT, transferrin saturation.

* Corresponding author at: Laboratory of experimental Medicine, Hospital Alemán, School of Medicine, University of Buenos Aires, Av. Pueyrredon 1640, 1118 Buenos Aires, Argentina.
E-mail address: jorgetoblli@fibertel.com.ar (J.E. Toblli).

http://dx.doi.org/10.1016/j.ijcard.2016.03.039
0167-5273/

studies suggest an increased generation of reactive oxygen species (ROS) as well as reactive nitrogen species (RNS) in heart failure [7]. Indeed, the important role of oxidative/nitrosative stress in the pathophysiological mechanism of LV remodeling responsible for HF progression is increasingly being recognized. Among others, oxidative/nitrosative stress can cause contractile failure and structural damage in the myocardium [7]. Moreover, by affecting directly the myocardial cellular structure and function or by activating integral signaling molecules that contribute to myocardial remodeling and failure, oxidative/nitrosative stress contributes to a phenotype characterized by hypertrophy and apoptosis in isolated cardiac myocytes [8]. Interestingly, both IDA and ID have been shown to increase oxidative/nitrosative stress in the heart leading to aberrant mitochondrial and irregular sarcomere organization and cytochrome *c* release [9]. It has been suggested that the IDA-induced oxidative/nitrosative stress results from increased mitochondrial and enzymatic superoxide ($O_2^{\bullet -}$) production, and enhanced inducible nitric oxide synthase (iNOS) expression, and thus peroxynitrite ($ONOO^-$) formation [9].

Studies with iron-deficient animals suggested that intravenous (i.v.) iron treatment induces positive changes in the LV architecture and function [6] possibly by activating molecular pathways, which protect the heart and prevent myocardial remodeling [9]. Moreover, recent clinical trials with i.v. iron indicated that correction of ID and/or IDA has favorable outcomes on cardiac function in iron-deficient patients [10–12]. However, the underlying factors contributing to the positive outcomes of i.v. iron therapy in HF are not known. In this study we evaluated the effects of i.v. iron sucrose (IS) treatment on IDA-induced morphological and functional changes in the LV and the effect of i.v. iron sucrose on IDA-induced oxidative/nitrosative stress, proinflammatory, and repair process markers in the heart.

2. Methods

2.1. Animals and treatments

The investigation conforms to the Guide for the Care and Use of Laboratory Animals published by the US National Institutes of Health (NIH Publication No. 85-23, revised 1985). All animal experiments were approved by Animal Care Committee of Hospital Alemán, Buenos Aires, Argentina.

Thirty-six male Sprague–Dawley rats were divided into three groups ($n = 12$) as indicated in Fig. 1. After weaning, the non-anemic control group received standard rat chow (Universal Basal Diet, TestDiet Formula #5755, PMI International, Richmond, IN, USA) with normal iron content (60 ppm) for 16 weeks. The two other groups were made anemic by feeding them Low-Iron Purified Diet (10 ppm; TestDiet, Formula #5859, PMI International, Richmond, IN) for 16 weeks. Hemoglobin (Hb) was assessed monthly by HemoCue (HemoCue, Ängelholm, Sweden) in all groups. The start of the treatment phase was denoted day 0. The i.v. iron treatment group (IDA + IS) received weekly administrations of iron sucrose [Venofer®; lot 517100, Vifor (International Inc.), St. Gallen, Switzerland] at a dosing 10 mg iron/kg body weight. The non-anemic control group (Control) and anemic group (IDA) received weekly administrations of i.v. saline solution at an equivalent volume. All groups continued with their corresponding diet schedule during treatment phase. Hb, serum iron, and transferrin saturation (TSAT) were evaluated on day 0 before IS/saline administration (baseline) and on day 29. Blood samples were collected from the tail vein in capillary tubes after 14 h of fasting. At the end of the study, 24 h after the last i.v. injection (day 29), blood samples were collected and rats were sacrificed by subtotal exsanguination under anesthesia (sodium thiopental 40 mg/kg body weight intraperitoneal) according to institutional guidelines for animal care and use. The heart of each rat was perfused with ice-cold saline through the abdominal aorta until free of blood and removed for further analyses.

2.2. Hemoglobin, serum iron and transferrin saturation

Hemoglobin (Hb) was determined by SYSMEX XT 1800i Roche Diagnostic. Serum iron was assessed by colorimetric method using an Autoanalyzer Modular P800 Roche Diagnostic with the corresponding reagents (Roche Diagnostic GmbH, Mannheim, Germany). Transferrin saturation (TSAT) was calculated using the following equation: Serum iron concentration/total iron-binding capacity/100 = TSAT (%) [13–15].

2.3. Echocardiographic measurements

Echocardiographic evaluation of LV was conducted as described previously [16]. Briefly, transthoracic echocardiograms were obtained without anesthesia by a echocardiographic system (Toshiba Corporation, Tokyo, Japan) with 5–8 MHz phased array transducer at baseline and at the end of the experiment. M-mode and bidimensional echocardiography was performed in minor axis at the level of papillary muscle. The thickness of the interventricular septum (IVS) and the left ventricular posterior wall in diastole (LVPW) were determined in the short axis at the midchordal level. LV dimensions, end-diastolic (LVDd) and end-systolic (LVSd), were measured perpendicularly to the short axis of the ventricle at the midchordal level. Fractional shortening (FS) was calculated as FS = (end-diastolic dimension − the end-systolic dimension) / end-diastolic dimension. The peak of systolic wave (S wave) and early diastolic filling (E wave) was also analyzed by color tissue Doppler imaging of left ventricular posterior wall (short axis). Velocity was expressed as cm/s. Left ventricular mass (LVM) was determined using the standard cube method.

2.4. Oxidative stress parameters in the heart

Fractions of the left ventricular wall were homogenized (1:10, w:v) in 0.05 M sodium phosphate buffer (pH 7.4). Malondialdehyde (MDA) was assessed directly from the homogenate to evaluate lipid peroxidation by thiobarbituric acid reactive species (TBARS) [17]. Catalase activity was measured in the resulting supernatant after centrifuging part of the homogenate for 15 min at 4 °C and 9500 ×*g* [18]. Further fractions were homogenized (1:3, w:v) in ice cold 0.25 M sucrose solution. Glutathione (GSH) levels were determined in the 10,000 ×*g* supernatant [19,20]. The supernatant obtained after centrifugation at 105,000 ×*g* for 90 min was used for measuring Cu,Zn superoxide dismutase (Cu,Zn-SOD) and glutathione peroxidase (GPx) activities [21,22]. Enzyme units (U) were defined as the amount of enzyme producing 1 nmol of product or consuming 1 nmol of substrate (catalase) under the standard incubation conditions. Specific activity was expressed as U/mg protein. One unit of Cu,Zn-SOD was defined as the amount of Cu,Zn-SOD capable of inhibiting the rate of NADH oxidation by 50% of that measured in the control.

2.5. Western blotting and densitometric analysis

Tissue samples from LV and interventricular septum were solubilized in 1% Triton detergent and analyzed by Western blotting as described previously [23]. For assessing nitrosative stress, polyvinyl difluoride membranes with transferred proteins were probed with anti-nitrotyrosine antibody at dilution 1:2000 (AB5411, Millipore, Billerica, MA, USA). Inflammatory response was evaluated by probing for anti-tumor necrosis factor-α (TNF-α; AF-510-NA, R&D Systems, Minneapolis, MN, USA) at a dilution 1:1000, with anti-p65 subunit of nuclear factor κB (NFκB p65; sc-8008, Santa Cruz Biotechnology, USA) at a dilution 1:1000, and with anti-phospho-NF-κB p65 (p-NFκB p65; sc-101748, Santa Cruz Biotechnology, USA) at a dilution 1:1000. Repair response was assessed with anti-heat shock protein 27 (HSP 27; sc-1048, Santa Cruz Biotechnology, USA) and with anti-HSP 70 (HSP 70, sc-1060, Santa Cruz Biotechnology, USA), both at a dilution 1:1000.

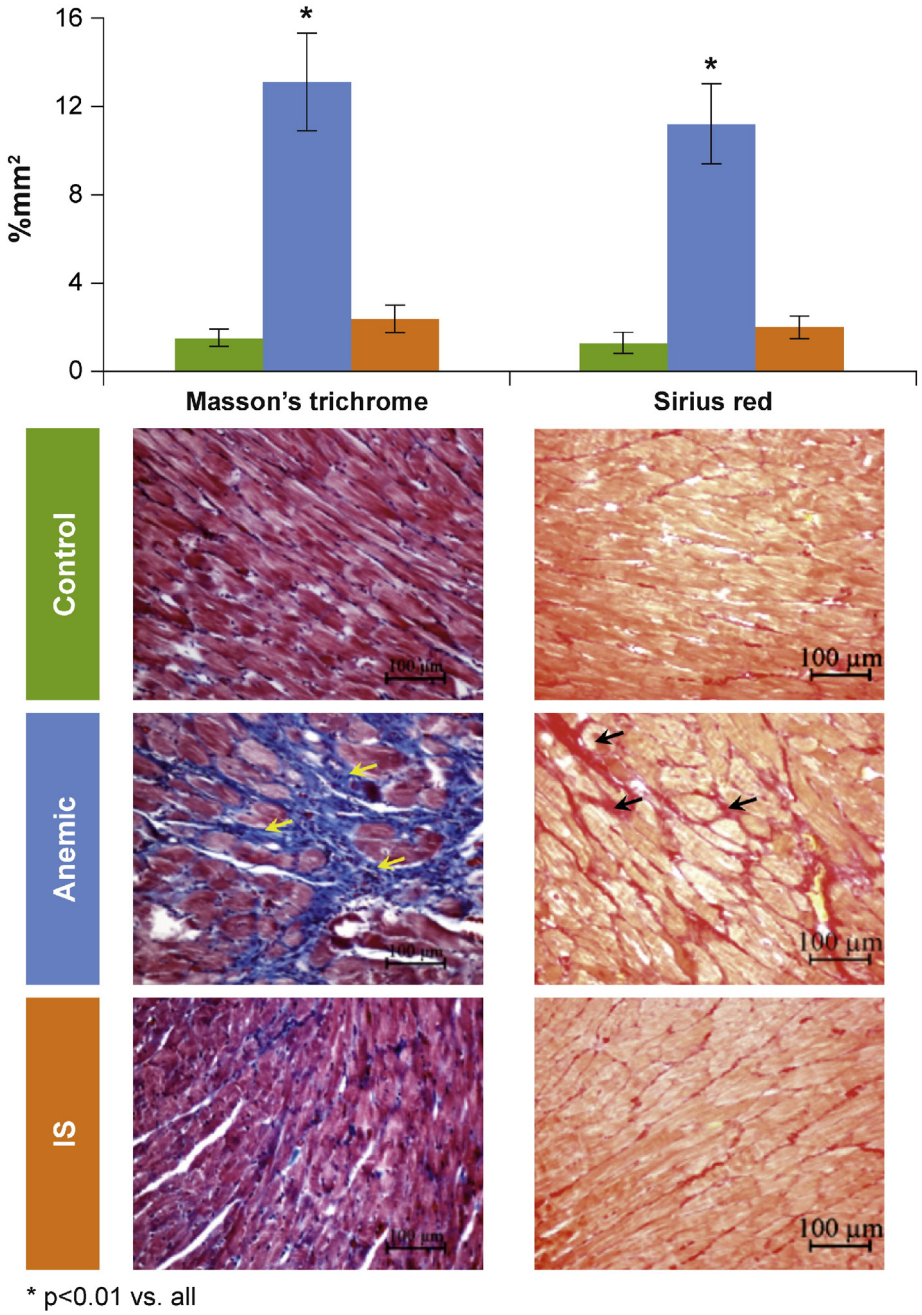

Fig. 1. Myocardial extracellular volume expansion (Masson's trichrome) and cardiac fibrosis (Sirius Red) in left ventricle and interventricular septum at the end of treatment (day 29). Data are expressed as mean ± SD. *p < 0.01 vs. all groups.

Heme oxygenase-1 (HO-1) was evaluated by anti-HO-1 (HO-1, sc-1796, Santa Cruz Biotechnology) at a dilution 1:1000. After washing, membranes were probed with a HRP-conjugated goat anti-rabbit secondary antibody at dilution 1:20,000 (sc-2004, Santa Cruz Biotechnology, Santa Cruz, CA, USA). Specific bands were detected by enhanced chemiluminescence (ECL; Amersham, Piscataway, NJ, USA). Autoradiographs were scanned and band intensities were quantified by digital densitometry using Gel-Pro Analyzer 4.0 software (Media Cybernetics, Silver Spring, MD, USA). The data was recorded as mean optical density intensity. Equal protein loading of samples was confirmed by stripping PVDF membranes with a commercial Re-blot solution (Chemicon, Billerica, MA) and then re-probing with anti-β-actin primary antibody (A5316, Sigma-Aldrich, St. Louis, MO) at a dilution 1:5000; and HRP-conjugated goat anti-mouse secondary antibody (dilution 1:20,000; cat. no. sc-2005, Santa Cruz Biotechnology) followed by chemiluminescent detection and densitometric quantification as described above.

2.6. Light microscopy, immunohistochemistry and histomorphometry

Fragments from left ventricle and interventricular septum were fixed in phosphate-buffered 10% formaldehyde (pH 7.2) and embedded in paraffin. Three micron sections were cut and stained with hematoxylin-eosin, Masson's trichrome and Sirius Red to evaluate extracellular expansion and fibrosis [24]. Immunostaining was carried out using a modified avidin–biotin-peroxidase technique (Vectastain ABC kit, Universal Elite, Vector Laboratories, CA, USA) as described previously [25]. Immunohistochemistry was performed with the same antibodies as for Western Blot analysis: TNF-α at a dilution 1:100, NF-κB p65, HSP

27 at a dilution 1:200, HSP 70 at a dilution 1:200, nitrotyrosine at a dilution 1:100and HO-1 at a dilution 1:100. Histomorphometric observations were performed with a light microscope (Nikon E400, Nikon Instrument Group, Melville, New York. USA) at × 400 magnification, and with image analyzer (Image-Pro Plus 4.5 for Windows, Media Cybernetics LP, Rockville, MD). In all cases, two independent observers performed a blinded fashion evaluation. All results for histological staining were expressed as mean percentage of positive immunostaining/mm^2 from ten random images viewed and evaluated.

2.7. Statistics

Values were expressed as mean ± SD. All statistical analyses were performed using absolute values and processed through GraphPad Prism, version 6.00 for Windows (GraphPad Software Inc., La Jolla, CA, USA). The assumption test to determine the Gaussian distribution was performed by the Kolmogorov and Smirnov method. For parameters with Gaussian distribution, comparisons among groups were carried out using ANOVA; for those parameters like histological data with non-Gaussian distribution comparisons were performed by Kruskal–Wallis test (nonparametric ANOVA) and Dunn's multiple comparison test. A value of $p < 0.05$ was considered significant.

3. Results

3.1. Hemoglobin, serum iron and transferrin saturation

Animals fed with low iron diet for 16 weeks became anemic as indicated by a significant ($p < 0.01$) reduction in serum iron, TSAT, and Hb levels in comparison with rats fed with normal diet (Table 1).

Whereas anemia in the IDA group was slightly worsened by day 29 compared to the baseline, rats treated with IS showed increased Hb values, although not equivalent to the Hb values of the control group. Similarly, serum iron and TSAT values were significantly increased ($p < 0.01$) in IS-treated animals compared to untreated anemic animals on day 29, but did not reach those of the non-anemic control group (Table 1).

3.2. Echocardiography and tissue Doppler of the left ventricle

At baseline, i.e. after 16 weeks of low iron diet, before i.v. iron treatment, echocardiographic as well as tissue Doppler evaluation showed significant differences ($p < 0.01$) between untreated anemic and non-anemic control animals (Table 2). Anemic animals presented significantly increased ($p < 0.01$) LVDd, LVSd and LVPW. In addition, untreated anemic animals presented significant alterations ($p < 0.01$) in systolic and diastolic properties as expressed by lower velocity in S and E waves, respectively. Moreover, FS was also diminished in untreated anemic rats ($p < 0.01$). Notably, both LVM and heart rate were also significantly higher ($p < 0.01$) in the groups with IDA in comparison to the control group.

Table 1
Hematological parameters.

Group	Control	IDA	IS
Baseline (day 0)			
Hb (g/dl)	14.4 ± 0.5*	8.1 ± 0.6	7.9 ± 0.6
Serum iron (μg/dl)	224.0 ± 22.3*	48.7 ± 18.0	46.3 ± 20.9
TSAT (%)	41.5 ± 3.1*	12.2 ± 2.1	11.8 ± 2.6
End of treatment (day 29)			
Hb (g/dl)	14.6 ± 0.5	7.8 ± 0.5*	11.7 ± 0.7#
Serum iron (μg/dl)	225.9 ± 21.7	36.0 ± 14.5*	179.6 ± 19.9#
TSAT (%)	42.2 ± 2.9	9.2 ± 2.0*	25.6 ± 4.7#

Hb, hemoglobin; TSAT, transferrin saturation.
* $p < 0.01$ versus all groups,
\# $p < 0.01$ versus control.

Table 2
Cardiac morphology and function.

Group	Control	IDA	IS
Baseline (day 0)			
Heart rate (bpm)	370 ± 11*	397 ± 10	399 ± 11
LVSd (mm)	3.59 ± 0.06*	4.95 ± 0.07	4.98 ± 0.16
LVDd (mm)	7.78 ± 0.11*	8.00 ± 0.08	8.02 ± 0.09
LV PW (mm)	1.54 ± 0.04*	1.80 ± 0.06	1.79 ± 0.06
IVS (mm)	1.53 ± 0.04*	1.82 ± 0.05	1.80 ± 0.05
FS (%)	53.8 ± 1.0*	38.1 ± 1.1	37.9 ± 2.2
LVM (g)	0.67 ± 0.03*	0.88 ± 0.03	0.87 ± 0.04
S wave cm/s	33.0 ± 2.4*	23.7 ± 3.5	24.1 ± 3.9
E wave cm/s	61.7 ± 2.2*	40.7 ± 3.1	41.5 ± 3.5
End of treatment (day 29)			
Heart rate (bpm)	374 ± 12	415 ± 12*	385 ± 11
LVSd (mm)	3.57 ± 0.10	5.09 ± 0.08*	3.93 ± 0.13#
LVDd (mm)	7.78 ± 0.14	8.10 ± 0.09*	7.82 ± 0.06#
LV PW (mm)	1.55 ± 0.05	1.81 ± 0.06*	1.68 ± 0.05#
IVS (mm)	1.54 ± 0.03	1.82 ± 0.05*	1.74 ± 0.06#
FS (%)	54.8 ± 1.5	37.0 ± 1.2*	49.7 ± 1.6#
LVM (g)	0.68 ± 0.03	0.90 ± 0.03*	0.78 ± 0.02#
S wave cm/s	34.5 ± 3.5	22.3 ± 32*	30.7 ± 3.6#
E wave cm/s	62.4 ± 2.0	35.4 ± 4.2*	58.4 ± 4.0#
HW:BW (g/kg)	2.6 ± 0.2	4.1 ± 0.4*	3.1 ± 0.1#
Cardiomyocyte size (μm)	20.7 ± 1.0	28.5 ± 2.2*	23.2 ± 1.3#

BW, body weight; FS, fractional shortening; HW, heart weight; IVS, interventricular septum; LV PW, left ventricular posterior wall in diastole; LVM, left ventricular mass; LVDd, end-diastolic dimension of the left ventricle; LVSd, end-systolic dimension of the left ventricle.
* $p < 0.01$ versus all groups,
\# $p < 0.05$ versus control.

At the end of the study (day 29) IS-treated rats showed, although partial with respect to the control group, significant improvements ($p < 0.01$) in all evaluated echocardiographic and tissue Doppler variables compared to baseline values. In contrast, the untreated anemic animals (IDA group) presented similar or slightly worsened values vs baseline (Table 2). Both LVDd and LVSd as well as LVPW and IVS were significantly reduced ($p < 0.01$) in animals treated with IS compared to untreated anemic animals. Heart rate and LVM were both significantly lower ($p < 0.01$) in IS-treated than in untreated anemic animals. Treatment with IS also increased significantly ($p < 0.01$) FS, as well as S and E wave velocities (Table 2).

3.3. Heart weight and cardiomyocyte size

At the end of the experiment (day 29), animals of the IDA group presented with significantly increased ($p < 0.01$) heart weight and cardiomyocyte size compared to IS-treated animals and the control group (Table 2). Administration of IS partially prevented cardiac remodeling of cardiomyocytes and increase in the heart weight.

3.4. Extracellular expansion and fibrosis in the left ventricle and interventricular septum

On day 29, extracellular expansion and fibrosis in LV and interventricular septum were significantly increased ($p < 0.01$) in untreated anemic animals compared to control and IS-treated animals (Fig. 1).

3.5. Oxidative/nitrosative stress markers in the left ventricle and interventricular septum

At the end of the study (day 29), animals of the IDA group showed significantly ($p < 0.01$) higher levels of lipid peroxidation in the left ventricle and interventricular septum than the control and IS-treated group (Table 3). Activity of the antioxidant enzyme catalase was significantly reduced ($p < 0.01$) whereas that of Cu,Zn-SOD and

Table 3
Oxidative stress parameters in the left ventricle at the end of treatment (day 29).

Group	Control	IDA	IS
MDA (nmol/mg prot.)	0.8 ± 0.2	2.5 ± 0.6*	1.0 ± 0.3
Catalase (U/mg prot.)	25.8 ± 3.5	20.6 ± 1.8*	27.3 ± 2.7
Cu,Zn-SOD (U/mg prot.)	10.6 ± 1.0	14.9 ± 0.9*	11.5 ± 1.2
GPx (U/mg prot.)	154.2 ± 21.4	371.4 ± 38.2*	211.5 ± 25.3#
GSH:GSSG	6.5 ± 0.9	3.3 ± 0.6*	5.1 ± 0.5#

Cu,Zn-SOD, Cu,Zn superoxide dismutase; GPx, glutathione peroxidase; GSH:GSSG, ratio of reduced glutathione to oxidized glutathione; MDA, Malondialdehyde.
* $p < 0.01$ vs. all groups,
# $p < 0.01$ versus control.

GPx was significantly increased ($p < 0.01$) in untreated anemic animals compared to control animals and to those treated with IS. The ratio of reduced glutathione to oxidized glutathione (GSH:GSSG) was significantly reduced in untreated anemic animals compared to control and IS treated animals.

HO-1 was significantly increased ($p < 0.01$) in abundance (Fig. 2A) with large area of positive immunostaining (Fig. 2B) in untreated anemic animals compared to the non-anemic control group. In contrast, IS-treated animals showed similar results for HO-1 as the control group (Fig. 2). Similarly, tyrosine nitration was increased significantly ($p < 0.01$) in abundance (Fig. 2A) along with positive immunostaining (Fig. 2B) in untreated anemic animals compared to control animals.

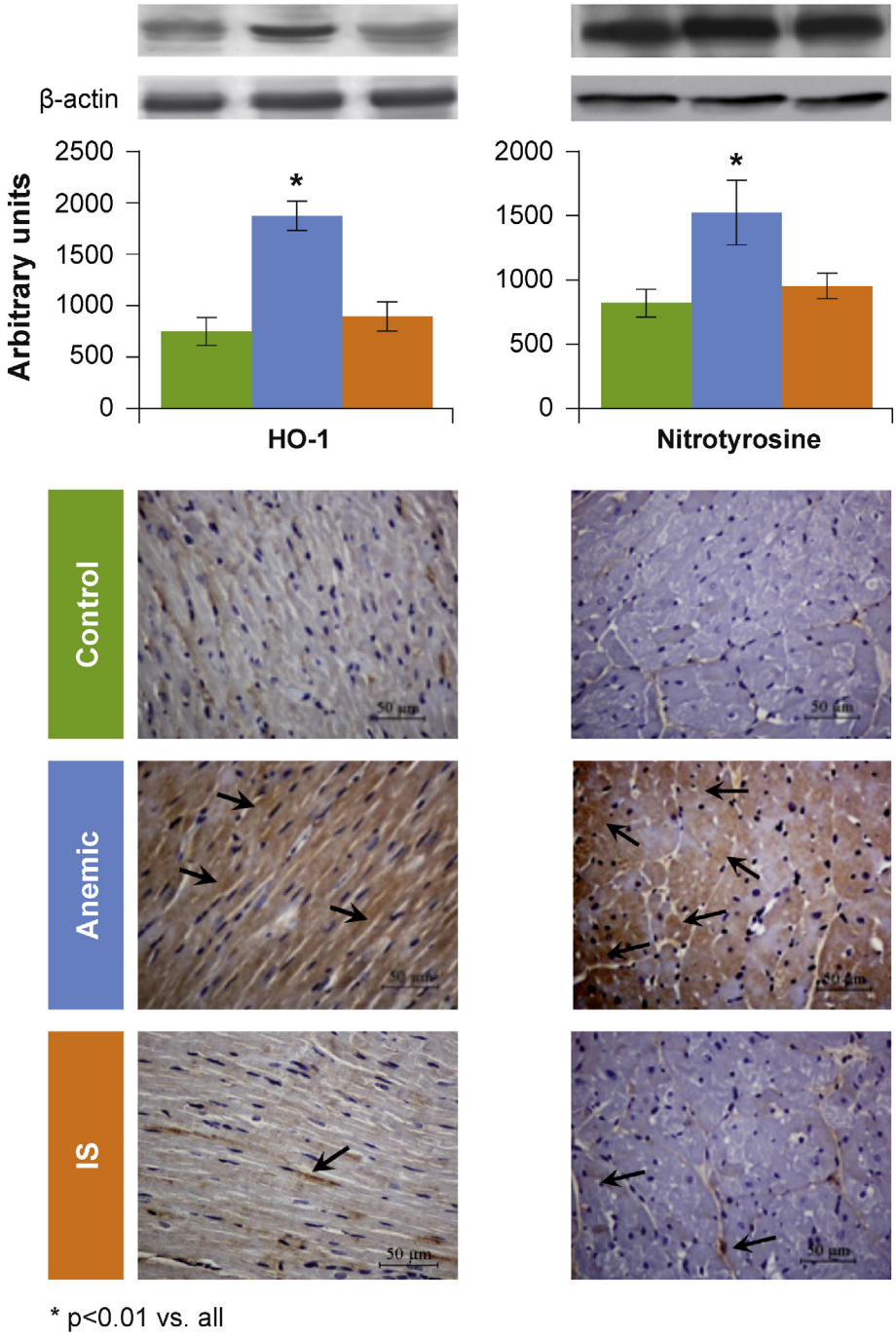

Fig. 2. Abundance (A) and localization (B) of heme oxygenase-1 (HO-1) and nitrotyrosine in left ventricle and interventricular septum at the end of treatment (day 29). Data are expressed as mean ± SD. *$p < 0.01$ vs. all groups.

Whereas IS-treated animals presented similar nitrotyrosine levels (Fig. 2A) and immunostaining (Fig. 2B) as the non-anemic control animals.

3.6. Pro-inflammatory markers

In order to evaluate the inflammatory response associated with anemia, protein abundance and phosphorylation levels of NF-κB$_{65}$ in LV and interventricular septum were assessed by Western Blot. Anemic animals displayed a significant increase ($p < 0.05$) in the abundance of NF-κB$_{65}$ compared to the non-anemic control animals and animals treated with IS (Fig. 3A), which was also visible by immunostaining (Fig. 3B). In addition, anemic animals also showed significantly increased ($p < 0.05$) phosphorylation of NF-κB$_{65}$ compared to the non-anemic control animals and the IS group (Control: 93.3 ± 25.7; IDA: 168.0 ± 11.3; IS: 110.0 ± 13.1; arbitrary units).TNF-α expression in LV and interventricular septum was also significantly increased ($p < 0.05$) in untreated anemic animals versus control and IS-treated animals as indicated by Western blots (Fig. 3A) and immunostaining (Fig. 3B).

3.7. Repair process markers

The repair process markers HSP27 and HSP70 were both significantly increased ($p < 0.01$) in untreated anemic animals, not only in abundance (Fig. 3A) but also in extent (Fig. 3B) compared to control and IS-treated animals on day 29.

4. Discussion

4.1. Major findings of the study

As expected, IS administration to anemic rats increased Hb levels, serum iron and TSAT. In addition, the treatment with IS showed significant improvement, in both cardiac morphology (reduced heart weight, decreased cardiomyocyte size, fibrosis), and function (echocardiographic findings). This improvement was associated with a significant decrease in oxidative stress (TBARS and GSH levels; CuZnSOD and GPx activities), nitrosative stress (HO-1 and nitrotyrosine abundance), inflammation (NF-κB$_{65}$ phosphorylation and abundance, TNF-α levels) as well as the markers of repair process (HSP27 and HSP70 levels) in cardiac tissue.

4.2. Echocardiographic and morphological findings

Iron deficiency, with or without anemia, has been suggested to trigger cardiovascular diseases, such as cardiac hypertrophy and CHF [5]. In developing rats, IDA has been shown to induce LV eccentric hypertrophy [6,26–29], together with distinct cellular degeneration and interstitial fibrosis [6,30]. Both clinical [10–12] and nonclinical [6,9] results suggest that correction of ID and/or IDA with i.v. iron has favorable outcomes on cardiac function. Although iron content seems to play an important role in the regulation of cardiovascular function and morphology, the mechanisms responsible for ID- and IDA-induced changes in the heart are still poorly understood.

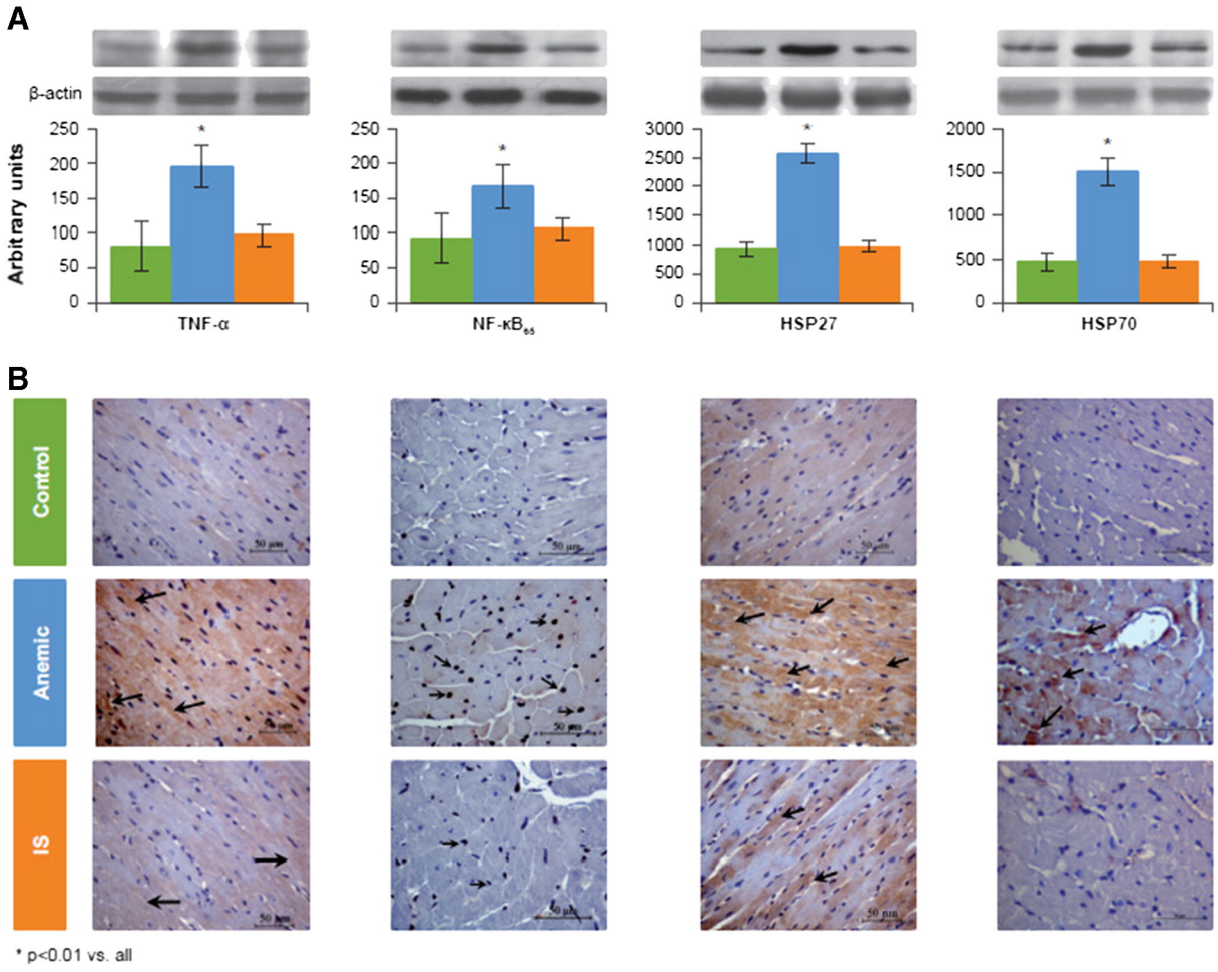

Fig. 3. Abundance (A) and localization (B) of proinflammatory markers (TNF-α and NF-κB$_{65}$) and repair process markers (HSP27 and HSP70) in left ventricle and interventricular septum at end of treatment (day 29). Data are expressed as mean ± SD. *$p < 0.01$ vs. all groups.

Echocardiographic and morphological findings of our study revealed IDA-induced cardiac hypertrophy and dysfunction in addition to IDA-induced oxidative/nitrosative stress and inflammation after 20 weeks of low iron diet, which is in line with prior nonclinical as well as clinical studies [5,9,31,32]. Iron is essential for the activity of many enzymes, including the enzymes of the mitochondrial electron transport chain, NADPH oxidase, nitric oxide synthases (NOSs) and enzymes with antioxidant activities. Lack of iron due to IDA leads to oxidative/nitrosative stress [34], which potentially plays a central role in IDA-induced cardiac damage [9]. Interestingly, a four-week treatment with i.v. iron sucrose (10 mg iron/kg body weight/week) improved cardiac morphology and function as well as attenuated IDA-induced oxidative/nitrosative stress and inflammation, without completely correcting the anemia. However, these results are well in line with the suggestion that i.v. iron treatment is able to restore the function of iron as an essential component of the enzymes involved in the energy metabolism very fast [33] thus, reducing IDA-induced oxidative/nitrosative stress. Furthermore, our results also support the recent clinical data showing that i.v. iron improves functional status, quality of life, and exercise capacity in iron-deficient CHF patients [10–12].

4.3. Potential mechanisms behind the beneficial effects of i.v. iron sucrose

Failing myocardium exhibits chronic activation of both pro-inflammatory cytokine expression [35] and NF-κB activation [36,37]. Chronic NF-κB activity in the murine failing heart is primarily related to p65 activation in myocytes, which is an absolute requirement for the up-regulation of the proinflammatory cytokines TNF-α, IL-1β, and IL-6 [38]. However, sustained p65 activation in myocytes reduces survival and promotes post-infarction LV remodeling, conveying profibrotic, proinflammatory, and proapoptotic effects [38]. We assessed two of these markers in the heart and showed that after 20 weeks of IDA the abundance and phosphorylation of cardiac p65 levels as well as TNF-α expression were increased. Consistent with the known profibrotic effects of both NF-κB and TNF-α [39], interstitial fibrosis, extracellular volume expansion and cardiac dysfunction were also observed in rats with IDA. Interestingly, besides attenuating increased cardiac TNF-α and p65 levels, i.v. iron sucrose treatment also ameliorated extracellular volume expansion and cardiac fibrosis, indicating that i.v. iron therapy can reduce or even prevent IDA-induced cardiac remodeling.

Expression of both HSP27 and HSP70 is increased in the early stage of cardiac remodeling in animal models [40] and play an important role in protecting the heart from oxidative stress [41,42]. In this study, we showed that alongside with elevated oxidative/nitrosative stress, HSP27 and HSP70 levels were also increased in the LV and interventricular septum of the untreated anemic rats. Interestingly, both HSP27 and HSP70 have been suggested to play a role in the regulation of iron homeostasis under oxidative stress conditions mainly by decreasing the levels of intracellular redox-active iron [43]. HSP70 has been shown to bind iron (II) in a non-redox active form under conditions simulating those of the lysosomal compartment, thus stabilizing lysosomes against oxidative stress [44].

4.4. Limitations

Although these results suggesting intravenous iron could be a promising therapeutic strategy for controlling IDA-induced cardiac damage, direct extrapolation of these data to human health and therapy could be inappropriate since this study has only been performed in rats under a specific experimental protocol.

5. Conclusion

Intravenous iron sucrose treatment of anemic rats reversed anemia-induced cardiac remodeling, prevented myocardial fibrosis, and improved cardiac function by attenuating oxidative/nitrosative stress and inflammation. The positive effects of i.v. iron sucrose treatment were evident in the heart even though anemia was not fully corrected. This is in agreement with previous data [43] showing that i.v. iron treatment is able to restore the function of iron as an essential component of various enzymes, thus normalizing the cellular iron homeostasis and restoring the cellular redox-balance.

Conflicts of interest

Professor Jorge E. Toblli has received research grants and consultancy fees from Vifor (International) Ltd. The other authors have no conflicts of interest to declare.

Acknowledgments

Scientific writing support was provided by Dr. Taija Koskenkorva-Frank (Vifor Pharma Ltd.). Support for graphics and illustrations were provided by Tracey Nichols (Tracey Nichols Graphic Design Ltd.).

References

[1] E. McLean, M. Cogswell, I. Egli, D. Wojdyla, B. de Benoist, Worldwide prevalence of anaemia, WHO vitamin and mineral nutrition information system, 1993–2005, Public Health Nutr 4 (2009) 444–454.
[2] R. Crichton, B. Danielson, P. Geisser, Iron Therapy with Special Emphasis on Intravenous Administration, fourth ed. UNI-MED Verlag AG, Bremen, 2008.
[3] R. Huch, R. Schaefer, Iron Deficiency and Iron Deficiency Anaemia, Thieme Medical Publishers, Pocket Atl. New York, 2006 1–80.
[4] G. Weiss, Iron metabolism in the anemia of chronic disease, Biochim Biophys Acta 1790 (2009) 682–693.
[5] E.A. Jankowska, S. von Haehling, S.D. Anker, I.C. Macdougall, P. Ponikowski, Iron deficiency and heart failure: diagnostic dilemmas and therapeutic perspectives, Eur Heart J 34 (2013) 816–829.
[6] Y. Naito, T. Tsujino, M. Matsumoto, T. Sakoda, M. Ohyanagi, T. Masuyama, Adaptive response of the heart to long-term anemia induced by iron deficiency, Am J Physiol Heart Circ Physiol 296 (2009) H585–H593.
[7] H. Tsutsui, S. Kinugawa, S. Matsushima, Mitochondrial oxidative stress and dysfunction in myocardial remodelling, Cardiovasc Res 81 (2009) 449–456.
[8] F.G. Spinale, M.L. Coker, C.V. Thomas, J.D. Walker, R. Mukherjee, L. Hebbar, Time-dependent changes in matrix metalloproteinase activity and expression during the progression of congestive heart failure: relation to ventricular and myocyte function, Circ Res 82 (1998) 482–495.
[9] F. Dong, X. Zhang, B. Culver, H.G. Chew Jr., R.O. Kelley, J. Ren, Dietary iron deficiency induces ventricular dilation, mitochondrial ultrastructural aberrations and cytochrome c release: involvement of nitric oxide synthase and protein tyrosine nitration, Clin Sci 109 (2005) 277–286.
[10] S.D. Anker, J.C. Comin-Colet, G. Filippatos, R. Willenheimer, K. Dickstein, H. Drexler, et al., Rationale and design of ferinject assessment in patients with iron deficiency and chronic heart failure (FAIR-HF) study: a randomized, placebo-controlled study of intravenous iron supplementation in patients with and without anaemia, Eur J Heart Fail 11 (2009) 1084–1091.
[11] P. Ponikowski, D.J. van Veldhuisen, J. Comin-Colet, G. Ertl, M. Komajda, V. Mareev, et al., Beneficial effects of long-term intravenous iron therapy with ferric carboxymaltose in patients with symptomatic heart failure and iron deficiency, Eur Heart J 36 (2015) 657–668.
[12] D.O. Okonko, A. Grzeslo, T. Witkowski, A.K. Mandal, R.M. Slater, M. Roughton, et al., Effect of intravenous iron sucrose on exercise tolerance in anemic and nonanemic patients with symptomatic chronic heart failure and iron deficiency FERRIC-HF: a randomized, controlled, observer-blinded trial, J Am Coll Cardiol 51 (2008) 103–112.
[13] J.E. Toblli, G. Cao, L. Oliveri, M. Angerosa, Effects of iron deficiency anemia and its treatment with iron polymaltose complex in pregnant rats, their fetuses and placentas: oxidative stress markers and pregnancy outcome, Placenta 33 (2012) 81–87.
[14] P. Fergelot, M. Ropert-Bouchet, E. Abgueguen, M. Orhant, M. Radosavljevic, G. Grimber, et al., Iron overload in mice expressing HFE exclusively in the intestinal villi provides evidence that HFE regulates a functional cross-talk between crypt and villi enterocytes, Blood Cells Mol Dis 28 (2002) 348–360.
[15] P. Youn, S. Kim, J.H. Ahn, Y. Kim, J.D. Park, D.Y. Ryu, Regulation of iron metabolism-related genes in diethylnitrosamine-induced mouse liver tumors, Toxicol Lett 184 (2009) 151–158.
[16] J.E. Toblli, G. Cao, C. Rivas, M.C. Muñoz, J.F. Giani, F.P. Dominici, et al., Cardiovascular protective effects of nebivolol in zucker diabetic fatty rats, J Hypertens 28 (2010) 1007–1019.
[17] W.G. Niehaus Jr., B. Samuelsson, Formation of malonaldehyde from phospholipid arachidonate during microsomal lipid peroxidation, Eur J Biochem 6 (1968) 126–130.
[18] B. Chance, A. Maehly, Assay of catalases and peroxidases, Methods Enzymol 2 (1955) 764–775.

[19] T.P. Akerboom, H. Sies, Assay of glutathione, glutathione disulfide, and glutathione mixed disulfides in biological samples, Methods Enzymol 77 (1981) 373–382.
[20] R. Rossi, E. Cardaioli, A. Scaloni, G. Amiconi, P. Di Simplicio, Thiol groups in proteins as endogenous reductants to determine glutathione-protein mixed disulphides in biological systems, Biochim Biophys Acta 1243 (1995) 230–238.
[21] E.M. de Cavanagh, F. Inserra, J.E. Toblli, I. Stella, C.G. Fraga, L. Ferder, Enalapril attenuates oxidative stress in diabetic rats, Hypertension 38 (2001) 1130–1136.
[22] D.R. Spitz, L.W. Oberley, Measurement of MnSOD and CuZnSOD activity in mammalian tissue homogenates, Curr Protoc Toxicol 7 (2001) (Unit7).
[23] J.F. Giani, M.M. Gironacci, M.C. Muñoz, C. Peña, D. Turyn, F.P. Dominici, Angiotensin-(1-7) stimulates the phosphorylation of JAK2, IRS-1 and akt in rat heart in vivo: role of the AT1 and mas receptors, Am J Physiol Heart Circ Physiol 293 (2007) H1154–H1163.
[24] M.L. Schuman, M.S. Landa, J.E. Toblli, L.S. Peres Diaz, A.L. Alvarez, S. Finkielman, Cardiac thyrotropin-releasing hormone mediates left ventricular hypertrophy in spontaneously hypertensive rats, Hypertension 57 (2011) 103–109.
[25] J.E. Toblli, G. Cao, C. Rivas, H. Kulaksiz, Heart and iron deficiency anaemia in rats with renal insufficiency: the role of hepcidin, Nephrology 13 (2008) 636–645.
[26] D.M. Medeiros, J.L. Beard, Dietary iron deficiency results in cardiac eccentric hypertrophy in rats, Proc Soc Exp Biol Med 218 (1998) 370–375.
[27] G. Olivetti, C. Lagrasta, F. Quaini, R. Ricci, G. Moccia, J.M. Capasso, et al., Capillary growth in anemia-induced ventricular wall remodelling in the rat heart, Circ Res 65 (1989) 1182–1192.
[28] G. Olivetti, F. Quaini, C. Lagrasta, R. Ricci, G. Tiberti, J.M. Capasso, et al., Myocyte cellular hypertrophy and hyperplasia contribute to ventricular wall remodelling in anemia-induced cardiac hypertrophy in rats, Am J Pathol 141 (1992) 227–239.
[29] Z. Tanne, R. Coleman, M. Nahir, D. Shomrat, J.P. Finberg, M.B. Youdim, Ultrastructural and cytochemical changes in the heart of iron-deficient rats, Biochem Pharmacol 47 (1994) 1759–1766.
[30] M.A. Rossi, S.V. Carillo, Electron microscopic study on the cardiac hypertrophy induced by iron deficiency anaemia in the rat, Br J Exp Pathol 64 (1983) 373–387.
[31] D.S. Silverberg, D. Wexler, A. Iaina, D. Schwartz, The role of correction of anaemia in patients with congestive heart failure: a short review, Eur J Heart Fail 10 (2008) 819–823.
[32] J.E. Toblli, C. Rivas, G. Cao, J.F. Giani, F. Funk, L. Mizzen, et al., Ferric carboxymaltose-mediated attenuation of doxorubicin-induced cardiotoxicity in an iron deficiency rat model, Chemother Res Pract 2014 (2014) 570241.
[33] W.T. Willis, K. Gohil, G.A. Brooks, P.R. Dallman, Iron deficiency: improved exercise performance within 15 hours of iron treatment in rats, J Nutr 120 (1990) 909–916.
[34] T.S. Koskenkorva-Frank, G. Weiss, W.H. Koppenol, S. Burckhardt, The complex interplay of iron metabolism, reactive oxygen species, and reactive nitrogen species: insights into the potential of various iron therapies to induce oxidative and nitrosative stress, Free Radic Biol Med 65C (2013) 1174–1194.
[35] S.D. Prabhu, B. Chandrasekar, D.R. Murray, G.L. Freeman, B-adrenergic blockade in developing heart failure: effects on myocardial inflammatory cytokines, nitric oxide, and remodelling, Circulation 101 (2000) 2103–2119.
[36] F. Grabellus, B. Levkau, A. Sokoll, H. Welp, C. Schmid, M.C. Deng, et al., Reversible activation of nuclear factor-kappaB in human end-stage heart failure after left ventricular mechanical support, Cardiovasc Res 53 (2002) 124–130.
[37] S.C. Wong, M. Fukuchi, P. Melnyk, I. Rodger, A. Giaid, Induction of cyclooxygenase-2 and activation of nuclear factor-kappaB in myocardium of patients with congestive heart failure, Circulation 98 (1998) 100–103.
[38] T. Hamid, S.Z. Guo, J.R. Kingery, X. Xiang, B. Dawn, S.D. Prabhu, Cardiomyocyte NF-kB p65 promotes adverse remodelling, apoptosis, and endoplasmic reticulum stress in heart failure, Cardiovasc Res 89 (2011) 129–138.
[39] D.L. Mann, Inflammatory mediators and the failing heart: past, present, and the foreseeable future, Circ Res 91 (2002) 988–998.
[40] Z. Li, Y. Song, R. Xing, H. Yu, Y. Zhang, Z. Li, et al., Heat shock protein 70 acts as a potential biomarker for early diagnosis of heart failure, PLoS One 8 (2013), e67964.
[41] P.T. Doulias, P. Kotoglou, M. Tenopoulou, D. Keramisanou, T. Tzavaras, U. Brunk, et al., Involvement of heat shock protein-70 in the mechanism of hydrogen peroxide-induced DNA damage: the role of lysosomes and iron, Free Radic Biol Med 42 (2007) 567–577.
[42] J. Wu, S. Jiang, Z. Ding, L. Liu, Role of heat shock protein 27 in cardiovascular disease, J Biochem Pharmacol Res 1 (2013) 43–50.
[43] H. Chen, C. Zheng, Y. Zhang, Y.Z. Chang, Z.M. Qian, X. Shen, Heat shock protein 27 downregulates the transferrin receptor 1-mediated iron uptake, Int J Biochem Cell Biol 38 (2006) 1402–1416.
[44] T. Kurz, U.T. Brunk, Autophagy of HSP70 and chelation of lysosomal iron in a non-redox-active form, Autophagy 5 (2009) 93–95.